Antenna System Optimization for Active Metamaterial-enhanced Magnetic Induction Communications

Zhangyu Li and Zhi Sun

Department of Electrical Engineering, University at Buffalo, State University of New York, Buffalo, NY 14260 E-mail: {zhangyul, zhisun}@buffalo.edu.

Abstract—Magnetic induction (MI) communication are widely used in applications in extreme environments, including environment surveillance, past disaster rescue, and resource detection since it does not suffer from high material absorption in lossy media. However, existing MI systems rely on high transmitting power and large antenna to reach practical communication range. Recently, metamaterial enhanced MI (M2I) communication was proposed, which can increase the signal strength of the original MI system to 30 dB in theory. However the latest practical implementation of M²I system only achieves an 8 dB gain due to the metamaterial loss. In this paper, the active metamaterial unit is introduced to the current M2I communication system to close the performance gap between theoretical and practical results. The antenna system is optimized based on the rigorously model of circuit, coil array structure and channel. Through analytical deduction and COMSOL simulations, the proposed active M²I antenna system shows significant power gain and improvement in communication range compared with the passive M²I system and the original MI system.

I. Introduction

In extreme environments, such as underwater and underground, EM wave-based wireless communication systems do not work due to the high path loss in the lossy media. Magnetic induction [1] (MI) communication partially addressed the problem by using magnetic field generated by coil antennas to carry information. The MI system need large antenna to efficiently transmit and receive the MI signal [8]. However, emerging applications in extreme environments, such as underground internet of things and underwater robotic swarms require strict size limitation (within 10 cm) of wireless transceivers to fit inside portable devices. The antenna efficiency becomes very low when the signals' wavelength is tens of meters, which caused limited communication range.

To address the aforementioned problem, metamaterials has been introduced in the metamaterial enhanced MI (M²I) communication system in [9], where an ideal metamaterial layer with negative permeability is used to enclose the original MI coil antenna. Through theoretical analysis, it shows that the MI signal strength can be enhanced by up to 30 dB under the assumption that the metamaterial shell is matched and without any loss. The practical implementation of the M²I system are investigated in [2]. However, the experimental result shows that the received signal strength of the practical M²I implementation is only about 8 dB higher than the original MI system. The key reason of the gap between theoretical prediction and practical performance is the metamaterial loss [9], which is caused by the resistance of the coil on the spherical array. This loss can dramatically impact the metamaterial enhancement in the M²I communications. Moreover, the geometry structure of coil array is not optimally

chosen in [2], which further enlarges the performance gap. In [5], Non-Foster Element circuit is first introduced to achieve re-configurable metamaterial gain, which is used for low-delay full-duplex M²I networks. However, [5] only introduces this concept without rigorous performance characterization and antenna system optimization. Several key questions need to be answered regarding active M²I system practical implementation: (1) How to quantitatively analyze the effects of active elements on the M²I transceivers and channel? How much enhancement in terms of power gain and communication range can be expected? (2) Given the same input power, can the M²I system with active elements still achieve better performance? (3) How to design the active spherical coil array? What is the optimal array geometric structure?

To answer all the questions, in this paper, we introduce the active metamaterials and optimally design the antenna system to realize the predicted performance bound in M²I communication. By adding negative resistance circuit in each coil unit's circuit on the spherical array, the metamaterial loss is reduced significantly. We develop an accurate circuit and channel model to rigorously characterize the end-toend communications. We investigate the influence of the geometry structure of the active spherical coil array on the M²I communication performance. We also find the circuit matching scheme to maximize the efficiency of the end-toend M²I signal transfer. Finally, we find the optimal active metamaterial coil array structure that achieves the highest signal strength enhancement with the best overall energy consumption efficiency. It should be noted that active elements also cost power, for fairly comparing, we use same total input power for all the systems. Through analytical deduction and COMSOL simulations, given the same input power, we prove the proposed active M²I antenna system achieves significant improvement in communication range compared with the passive M²I system and the original MI system.

The rest of the paper is organized as follows. In Section II, the architecture of active M^2I antenna system is explained. Then the circuit, spherical coil array, and channel of the active M^2I antenna system are analytically characterized in Section III. The active M^2I antenna system is optimized in Section IV. The paper is concluded in Section V.

II. ACTIVE M²I ANTENNA SYSTEM ARCHITECTURE

To address the problems in the existing practical design of M^2I antenna, we propose an active element-based M^2I antenna system. The system architecture is shown in Fig. 1. The Universal Software Radio Peripheral (USRP) devices are connected to the TX and RX antennas, respectively. At both

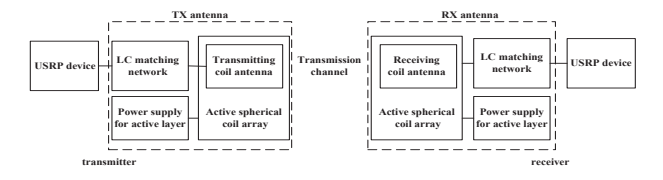


Fig. 1. Architecture of active M²I antenna system.

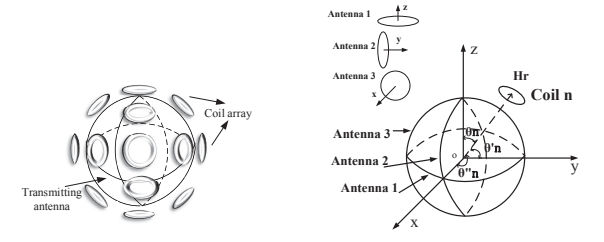


Fig. 2. M²I TX antenna.

Fig. 3. Tri-directional MI antenna.

the TX and RX sides, the LC matching networks connect the USRP devices and the MI antennas, which can ensure the largest power delivery to the load at receiver. Outside the transmitting and receiving antenna are the active spherical coil array, which can be treated as a layer of metamaterial to enhance the magnetic field generated by the coil antenna. The illustration of M²I TX antenna is in Fig. 2. Here we use tridirectional coil antenna [4] to ensure the omni-directionality, as shown in Fig. 3. Three identical coil antenna are orthogonal to each other. We define the direction of coil n is from the origin of spherical coordinate system to the center of coil n, and the angle of coil n's direction with z, y, x axis is θ_n , θ'_n , θ_n'' . The active element-based coil array used here can cancel the negative effect caused by the meta-loss. The active coil array on the TX and RX antennas are connected to the power supply.

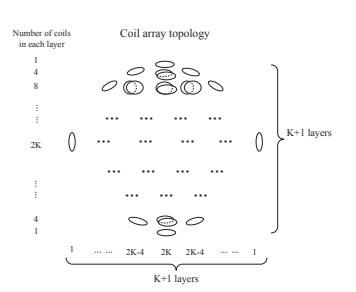
Through the whole system, we aim to find an optimal design that maximized the communication range of the system. This optimal design is determined by the whole system matching scheme, geometric structure of active coil array, and channel model together. The circuit and channel model are all related to the exact structure of active coil array. These topics are discussed elaborately in Section III.

III. Analytical Characterization of Active M^2I Antenna System

In this part, based on the system architecture in Fig. 1, we characterize the system through spherical coil array modeling, end-to-end circuit matching, and channel model analysis.

A. Geometric Structure of Spherical Coil Array

The spherical coil array is a transformed model of SRR (split resonant ring) array in [3]. When given a certain size of metamaterial sphere, the geometric structure of the coil array changes as the total number of coils changes. Hence, we need an analytical model to characterize the geometrical structure of the coil array. As shown in Fig. 4, the extension of Rhombicuboctahedron is used to model the geometrical structure of coil array. The coil array consists of K+1 (K is even number, K=2,4,6...) layers of coils, from the top to the bottom, left to right, or front to back. Except the layers on the



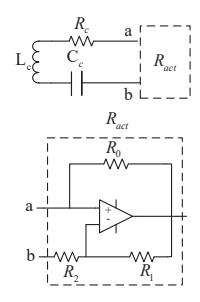


Fig. 4. Coil array configuration.

Fig. 5. Circuit model of coil unit and active element.

vertex, the coil number difference between any two adjacent layers is 4. All layers are in the same interval distance from each direction and all the coils are identical. Here we fix the diameter of spherical array as 10 cm for mobile device.

Based on this structure, the total number of the coils is $N = K^2 + 2$. Because the size of each coil varies when K is changed, we assume that the total area of all the coils is a constant when K varies in order to get the relation between coil unit's radius with K. Considering the intervals on the sphere, we fixed the total area for all the coils as 38 percent of the total area of the sphere. Then the radius of the coil unit changed with K is $a_K = \sqrt{\frac{0.0038}{K^2 + 2}}$ m. Each coil unit has one turn and is made of copper, the inductance of the coil circuit is $L_c^K = \sqrt{\frac{38}{K^2 + 2}} \times 3.15 \times 10^{-8} H$ [10]. While the ratio of inner and outer radius of the coil is fixed, the DC resistance of the coil is not changed with K. On the operating frequency, the AC resistance of the coil unit R_c^K is a constant when K varies. After getting the inductance and resistance, we can calculate the compensate capacity in each coil based on the operating frequency. Once the optimal K is derived, all the other parameters of the coil array are also decided.

B. Active Element Modeling

The configuration of active element circuit is shown in Fig. 5. The circuit of the active element consists of the resistance R_0 , R_1 , R_2 , and an ideal operation amplifier. The whole active element is equal to a negative resistance $R_{act} = -\frac{R_2}{R_1}R_0$, which is in series with the coil unit circuit with a resistance R_c , capacity C_c , and inductance L_c . The total impedance of coil circuit (varies with K) after adding the active element is $Z_c^K = R_c^K + j\omega L_c^K - \frac{j}{\omega C_c^K} + R_{act}$. When R_{act} is added, the current in the coil unit circuit can not be infinite. Hence $R_{active} > -R_c$ is required to keep the system stable. Although using active elements can enhance the performance of metamaterial layer, it also brings extra power consumption budget. Such trade-off is considered in the optimal design in section IV.

C. End-to-end Circuit Matching

The M^2I antenna system optimization need circuit matching scheme to maximize the power at the load when the source power is given. The equivalent end-to-end circuit model of the active M^2I antenna system is shown in Fig. 6. We need the conjugate impedance matching $Z_{in} = Z_S^*$ and $Z_{out} = Z_L^*$ [6], [7] to maximize the power at the load on the receiver. The whole circuit is modeled as the power source and the load connected

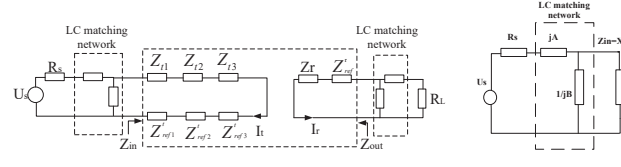


Fig. 6. End-to-end circuit model of $M^2 I$ antenna system.

Fig. 7. LC match-

to a two port network, while Z_{in} and Z_{out} are the input and output impedance of the two port network. The source and load impedance Z_S and Z_L only have resistance part if we use USRP to generate and analyze signal. While in the low operating frequency, the impedance of transmission line can be ignored, the matching scheme should be $Z_{in} = R_S$, $Z_{out} = R_L$. To achieve this matching, the LC matching network is used. One matching network is adding between the signal source and the M^2I TX antenna while another is adding between M^2I RX antenna and load.

In this circuit, U_S is the peak voltage of the source, I_t is the current in the transmitting coil antenna circuit, while I_r is the current in the receiving coil antenna circuit. For the tri-directional coil antenna, we have $Z_t = Z_{t1} = Z_{t2} = Z_{t3}$, which are the impedance of each coil antenna. When analyzing the receiver, we use one coil antenna instead of tri-directional antenna inside the coil array. Because a randomly placed tridirectional antenna is approximately equal to one coil antenna that is vertical to the incoming magnetic field in r direction [4]. Z_r is the impedance of the receiving coil circuit. On transmitter side, due to the symmetrical structure of coil array, we have $Z_{ref}^{l} = Z_{ref1}^{l} = Z_{ref2}^{l} = Z_{ref3}^{l}$, which is the reflection impedance on the transmitting antenna circuit from the coil array. And on receiver side, Z_{ref}^{r} is the reflection impedance coming from the coil array on receiving antenna circuit. In the practical case, Z_{in} is much larger than R_S , so the corresponding scheme of LC matching network used on the transmitter is shown in Fig. 7. The input resistance of the equivalent two-port network is $Z_{in} = 3(Z_t + Z_{ref}^t)$. Since the transmission distance is far enough, we can ignore the contribution of reflection impedance coming from the receiver. jA and $\frac{1}{iB}$ can be either a capacitance or inductance. The input impedance can be expressed in the complex form $Z_{in} = X + jY$, so B and A are calculated through

$$\begin{cases} B = \frac{Y \pm \sqrt{\frac{X}{R_S}} \cdot \sqrt{X(X - R_S) + Y^2}}{X^2 + Y^2} \\ A = \frac{1}{B} + \frac{YR_S}{X} - \frac{R_S}{BX}. \end{cases}$$
 (1)

When A and B are known, the exactly configuration of the LC matching network between transmitting antenna and signal source is decided. In the same way, the LC network on receiver side can be also derived.

D. Channel Modeling for Active M²I Communications

In this subsection, we establish the channel model of the active M^2I system to quantitatively characterize the enhancement of the active spherical coil array.

The illustration of the field distribution on transmitting side is shown in Fig. 8. The tri-directional MI antenna inside the coil array layer can be treated as magnetic infinitesimal. All the discussion later is in the spherical coordinate system. While for any coil on the spherical array, the *r* direction is vertical to the plane of the coil unit, Based on the LC matching scheme, the current in the transmitting coil antenna

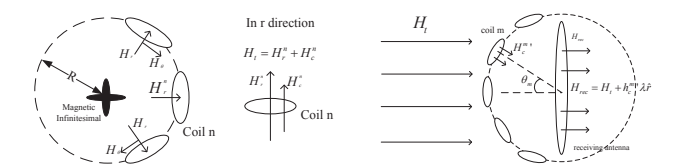


Fig. 8. The illustration of the field distribution on transmitting side, while the tri-directional MI antenna can be treated as ideal magnetic infinitesimal.

Fig. 9. The illustration of magnetic field distribution on receiving side.

is $I_t = \frac{U_s}{\sqrt{12R_s(Z_t + Z_{ref}^t)}}$. We define the coil unit's direction as r direction, which is vertical to its plane. Because the coil unit on the array is small enough compared to coil antenna in the center, all the magnetic filed in r direction can be regarded with the same angle θ . For arbitrary coil n on the coil array, the magnetic field on r direction can be expressed as

$$H_r^n = \frac{U_S}{\sqrt{12R_S(Z_t + Z_{ref}^t)}} \cdot \frac{jkR^2\hat{\Theta}_n}{2r^2} (1 + \frac{1}{jkr})e^{-jkr}\hat{r},$$
 (2)

where R is the radius of the coil antenna, k is the wave number in its transmitting medium, $\hat{\Theta}_n = \cos\theta_n + \cos\theta_n' + \cos\theta_n'' + \cos\theta_n''$, $Z_{ref}^t = \frac{\sum_{i=1}^N \omega^2 M_{ii}^2}{Z_r^K + j\omega \sum_{i=1,i\neq n}^N M_{in} \hat{\Theta}_i}$. Z_c^K is the impedance of the coil on the coil array, which is determined by K. M_{ti} is the mutual inductance between one of the coil antenna in the tridirectional transmitter and coil i. M_{in} is the mutual inductance between coil n and coil i. coil i is any other coil on the spherical array except coil n. The magnetic field in all the r direction can induce a current in the coil unit, we define the current in arbitrary coil n is I_n . In the position of coil n, not only the magnetic field from the transmitter but also the magnetic field generated by all the other coils' current can generate magnetic fields. Hence, we define the magnetic field caused by all the other coils on the position of coil n as H_r^n . While H_r^n and H_r^n are both in r direction, the total magnetic field at the position of coil n is defined as H_t . Based on the Kirchhoff's law and the definition of H_r^n , we have

$$\begin{cases} I_n Z_c^K = -j\omega\pi a_K^2 \mu_0 H_r^n - j\omega\pi a_K^2 \mu_0 H_c^n \\ -j\omega\pi a_K^2 \mu_0 H_c^n = -j\omega \sum_{i=1, i\neq n}^N M_{in} I_i, \end{cases}$$
(3)

where ω is the operating angle frequency, μ_0 is the permeability in vacuum, a_K is the radius of the coil unit.

By using (2) and (3), we can derived the total magnetic field from the position outside the coil n, which is

$$H_{t} = H_{r}^{n} + H_{c}^{n} = \frac{U_{S}}{\sqrt{12R_{S}(Z_{t} + Z_{ref}^{t})}} \cdot \frac{Z_{c}^{K}\hat{\Theta}_{n}^{2}}{Z_{c}^{K}\hat{\Theta}_{n} + j\omega\sum_{i=1, i\neq n}^{N} M_{in}\hat{\Theta}_{i}} \cdot \frac{jkR^{2}}{2r^{2}}(1 + \frac{1}{jkr})e^{-jkr}\hat{r}.$$
(4)

It should be noted that H_t is in the propagating field form, so we can derive the magnetic field at anywhere when r varies. At the receiver, there is also a spherical coil array, the same with one in the transmitter. We assume that the distance between the transmitter and receiver is far enough so that when H_t propagate at the receiver, it can be treated as plane wave as shown in Fig. 9. H_t is vertical to the receiving coil's plane, as discussed in Section III-C. On the active metamaterial layer at receiver, for arbitrary coil m, the magnetic field that can induce current on coil m is only from the component that is vertical to the coil unit's plane, which is $H_r \cos \theta_m$, where θ_m is the angle between the orientation of coil m to the receiving coil antenna's orientation. We define the magnetic field generated

by all the other coils except coil m on coil m's position as $H_c^{m\prime}$, we have

$$-j\omega\pi a_K^2 \mu_0 H_c^{m\prime} = -j\omega \sum_{i=1}^N M_{im} I_i, \qquad (5)$$

where M_{im} is the mutual inductance between any coil i on the coil array $(i \neq m)$ to coil m. And using Kirchhoff's law on the

$$I_m'Z_c^K = -j\omega\pi a_K^2\mu_0 H_t \cos\theta_m - j\omega M_{rm}I_r - j\omega\pi_K^2\mu_0 H_c^{m\prime}, \tag{6}$$

 $I'_m Z_c^K = -j\omega \pi a_K^2 \mu_0 H_t \cos \theta_m - j\omega M_{rm} I_r - j\omega \pi_K^2 \mu_0 H_c^{m'}$, (6) where Z_c^K is the total impedance of the coil unit, I'_m is the current in coil m, M_{rm} is the mutual inductance between the receiving coil antenna and coil m on the spherical array. The direction of $H_c^{m\nu}$ on different coil m 's position depends on $\cos \theta_m$, while only the component that is vertical to the plane cos θ_m , while only the component that is vertical to the plane of receiving antenna can generate emf (induced electromotive force) on the receiving coil. The sum of the projections of all the $H_c^{m\nu}$ on receiving coil's orientation is $\sum_{m=1}^{N} H_c^{m\nu} \cos \theta_m$, then all the effective components of all the $H_c^{m\nu}$ on the coil array is $\frac{\sum_{m=1}^{N} H_c^{m\nu} \cos \theta_m}{N}$. Due to the symmetrical structure of the coil array, the amplitude of each $H_c^{m\nu}$ is the same. Hence the total magnetic filed on the H_t direction can be expressed as

$$H_{rec} = H_t + \frac{h_c^{mr} \sum_{m=1}^{N} \cos \theta_m}{N} \cdot \hat{r}, \tag{7}$$

where h_c^{mr} is the amplitude of H_c^{mr} , \hat{r} is the orientation of H_t . The current at the receiving coil circuit after LC matching is

$$I_{r} = \frac{-j\omega\pi R^{2}\mu_{0}H_{rec}}{\sqrt{4R_{L}(Z_{r} + Z_{ref}^{r})}}.$$
 (8)

Combine (5), (6), (7), (8), the expression of H_{rec} in terms of the coming magnetic field H_t can be expressed as follows.

$$H_{rec} = H_t + h_c^{m'} \lambda \hat{r}$$

$$= H_{t} \left[1 - \frac{\lambda^{2} (\pi a_{K}^{2} \mu_{0} + \hat{M}_{rm} p) j \omega \sum_{i=1, i \neq m}^{N} M_{im} \cos \theta_{i}}{\lambda Z_{c}^{K} \pi a_{K}^{2} \mu_{0} + (\pi a_{K}^{2} \mu_{0} + p \lambda^{2} \hat{M}_{rm}) j \omega \sum_{i=1, i \neq m}^{N} M_{im} \cos \theta_{i}} \right],$$
(9)

where M_{ri} is the mutual inductance between the receiving coil antenna and any coil i on the spherical array. And $\lambda = \frac{\sum_{m=1}^{N} \cos \theta_m}{N}$, $p = \frac{-j\omega\pi R^2 \mu_0}{\sqrt{4R_L(Z_r + Z_{ref}^r)}}$, $Z_{ref}^r = \frac{\sum_{i=1}^{N} \omega^2 M_{ri}^2}{Z_c^K + j\omega \sum_{i=1, i \neq m}^{N} M_{im} \cos \theta_i}$, \hat{M}_{rm} can

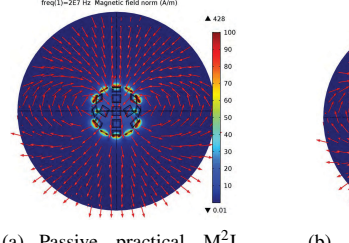
be derived by $\hat{M}_{rm} = \frac{\dot{M}_{rm}}{\cos \theta_m} \approx \frac{\mu_0 \pi a_K^2}{2R}$. Through (4) and (9), we establish the channel model of system so that the enhancement of active-element based metamaterial coil array with different total coil number can be analyzed.

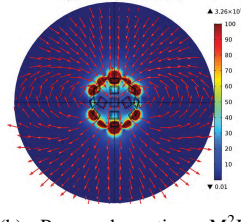
IV. OPTIMAL DESIGN OF ACTIVE M²I ANTENNA SYSTEM

Based on the exact channel model of the active M²I system, we can quantitatively evaluate the enhancement effects of the active metematerial layer. Then considering the overall power constraint, the exact structure of the coil array that achieves the largest communication range improvement can be derived.

A. Enhancement Analysis by The Active Metamaterial Layer

In active M²I antenna system, the receiving power at the load is $P_r = \frac{1}{2} I_L^2 R_L = \frac{emf^2}{8R_L}$, where I_L is the current on the load. $emf = -j\omega\pi R^2 \mu_0 H_{rec}$, when the operating frequency is fixed, P_r is positively related to the square of H_{rec} , so the receiving power P_r is proximized when the applitude of the receiving power P_r is maximized when the amplitude of H_{rec} is maximized given the fixed source power. In order to evaluate the enhancement of the active M^2I system, we use the original MI system for comparison. Except not having





(a) Passive practical M²I

(b) Proposed M^2I

Fig. 10. Simulation of magnetic field in near region in different systems.

the spherical coil array layer, the configuration of the original MI system is the same as the active M²I system, we assume that both the active M²I system and original MI system are already matched. The signal source power is set as $P_t = \frac{U_S^2}{4R_S}$. When the transmission distance is d, we define the magnetic field arriving at the receiver is H_{rec}^{MI} , and the magnetic field arriving at the entire M^{II} custom is II_{rec}^{MI} . The set of II_{rec}^{MI} . arriving at the receiver is H_{rec} , and the magnetic field arriving at the active M^2I system is $H_{rec}^{M^2I}$. Then, we define the enhancement gain of the active M^2I system over the original MI system on the magnetic field intensity as G. Hence, $G = \frac{h_{rec}^{M^2I}}{h_{rec}^{R}}$, where $h_{rec}^{M^2I}$ and h_{rec}^{MI} are the amplitudes of magnetic field $H_{rec}^{M^2I}$ and H_{rec}^{MI} , respectively. G can be derived based on (2) (4) (9) based on (2),(4),(9).

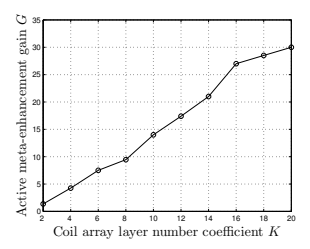
$$G = \sqrt{\frac{Z_{t}}{Z_{t} + Z_{ref}^{t}}} \cdot \left| \frac{Z_{c}^{K} \hat{\Theta}_{n}}{Z_{c}^{K} \hat{\Theta}_{n} + j\omega \sum_{i=1, i \neq n}^{N} M_{in} \hat{\Theta}_{i}} \cdot \left[1 - \frac{\lambda^{2} (\pi a_{K}^{2} \mu_{0} + \hat{M}_{rm} p) j\omega \sum_{i=1, i \neq m}^{N} M_{im} \cos \theta_{i}}{\lambda Z_{c}^{K} \pi a_{K}^{2} \mu_{0} + (\pi a_{K}^{2} \mu_{0} + p \lambda^{2} \hat{M}_{rm}) j\omega \sum_{i=1, i \neq m}^{N} M_{im} \cos \theta_{i}} \right].$$
(10)

The max value of G corresponds to the largest enhancement that the active M²I system can achieve over original MI system. G is a function of K, where K+1 is the layer number of the active coil array.

In practical case, K can not be infinitely large. Otherwise the circuit unit is too small to implement. Hence, we choose K varies from 2 to 20 (K is even number). The resonant frequency is selected at 20 Mhz. The resistance of the coil antenna is selected to be 0.1Ω . In this case, the relation between G and K is shown in Fig. 11. We can see that G increases with K, when K=20, the largest value of $G \approx 30$ achieves, so the best enhancement effect of the active M²I coil array achieves when K=20. It should be noted that the enhancement here does not consider the power consumption in the active coil layer, which will be discussed in next subsection. The COMSOL Multiphysics [11] simulation result in Fig. 10 shows that the enhancement effect of near region magnetic field intensity in active M²I transmitter side is prominent comparing with the passive M²I system, the frequency is set as 20Mhz and the array layer number is 7 here. The path-loss performance comparison of active M²I system with different geometric structures and the original MI system is given in Fig. 12, which shows the active M²I system can enhance the received signal by up to 30 dB in practical design.

B. End-to-end Performance Optimization for Active M²I Antenna System

For fairly comparing the communication range improvement over passive M²I and original MI system, we should con-



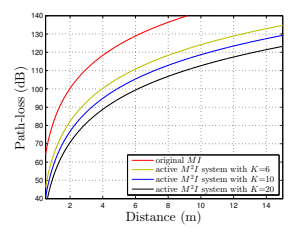


Fig. 11. The relation between the enhancement gain G and coil layer number coefficient K, the active coil array has K + 1 layers.

Fig. 12. Path-loss comparison between original MI and active M^2I system.

sider the overall power consumption, which contains source power used to drive the MI antenna (P_t) and the power consumed in the active elements (P_{act}) . When the overall power $(P_t + P_{act})$ is fixed, the more power we receive at the load, the larger communication range can be achieved.

The ratio of the received power at load (P_r) to the overall power of active M^2I system is defined as $\eta_{M^2I} = \frac{P_r}{P_1 + P_{act}}$, where η_{M^2I} is the overall power utilization rate in active M^2I system. P_{act} is the power that is consumed on the active elements on both the transmitter and receiver side, we have $P_{act} = \sum_{n=1}^{N} \frac{1}{2} I_n^2 |R_{act}| + \sum_{n=1}^{N} \frac{1}{2} I_m^{\prime 2} |R_{act}| + 2NP_{static}$, where P_{static} is the quiescent power of the amplifier in each active circuit. N is the total number of coils on the spherical coil array. I_n is the current in coil n on the coil array of the transmitting side while I_m' is the current in coil m on the spherical array of receiving side. Since $I_m' \ll I_n$, P_{act} can be expressed as

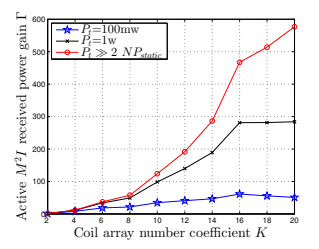
$$\begin{split} P_{act} &\approx \sum_{n=1}^{N} \frac{1}{2} I_{n}^{2} |R_{act}| + 2N P_{static} \\ &= P_{t} \sum_{n=1}^{N} \frac{\omega^{2} \hat{M}_{tn}^{2} |R_{act}|}{6(Z_{t} + Z_{ref}^{t}) \cdot (Z_{c}^{K} + j\omega \sum_{i=1, i \neq n}^{N} M_{in} \hat{\Theta}_{i})^{2}} + 2N P_{static}. \end{split} \tag{11}$$

Then we define the receiving power at the load of a well matched MI system is P_r^{MI} , the overall power consumed in MI system is only the source power P_t . Hence, the power utilization rate in original MI system is $\eta_{MI} = \frac{P_r^{MI}}{P_t}$. We can define Γ as the active M²I received power gain over original MI system when a fixed overall power is given, where

$$\Gamma = \frac{\eta_{M^2I}}{\eta_{MI}} = \frac{G^2}{1 + \frac{P_{act}}{P_c}}.$$
 (12)

When Γ is maximized, the largest communication range can be achieved. Γ is a function of coil array layer number coefficient K and source power P_t . In practical case, the operational amplifiers used here has $P_{static} \approx 2 \text{mW}$. At the resonant frequency, the relation between Γ and K with different source power P_t are shown in Fig. 13.

Considering a practical optimal design case (optimal design is chosen under constraint $K \le 20$) that the overall power is 34 dBm (source power P_t =1 W), the largest $\Gamma \approx 280$ achieves when K=16, so the optimal design is achieved when the active spherical array has a structure with 17 layers of coils. The received signal power at the load of receiver in active M^2I , passive M^2I and original MI system is shown in Fig. 14. The received power threshold for the system is about -110 dBm, so the communication range of the optimized M^2I antenna system can reach to about 28 m, which is a dramatically



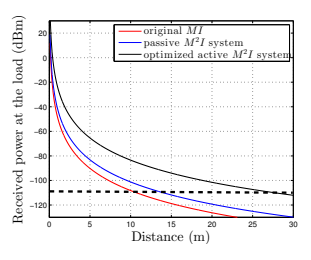


Fig. 13. The relation between Γ and K, Γ is the active M^2I received power gain over original MI system under a overall power, P_t is the source power.

Fig. 14. The received signal power at the load in active M²I, passive M²I and original MI system.

improvement over original MI system (9 m) and passive M²I system (12 m).

V. Conclusion

In this paper, we propose an optimized active element based M^2I antenna system design. After using the active elements and the matching scheme to the whole system, we establish an elaborate channel model to analyze the enhancement brought by the active metamaterial layer. Through analytical calculation, the structure of coil array that optimize the performance of the whole system is derived. The results show that the active M^2I antenna system with the optimized design can enhance the signal strength to extend the communication range to about 28~m, which is a dramatically improvement compared with practical passive M^2I system (12 m).

REFERENCES

- Z. Sun and I. F. Akyildiz, "Magnetic Induction Communications for Wireless Underground Sensor Networks," in IEEE Transactions on Antennas and Propagation, vol. 58, no. 7, pp. 2426-2435, July 2010.
- [2] H. Guo, Z. Sun and C. Zhou, "Practical Design and Implementation of Metamaterial-Enhanced Magnetic Induction Communication," in IEEE Access, vol. 5, pp. 17213-17229, 2017.
- [3] S. Hrabar, Z. Eres and J. Bartolic, "Capacitively Loaded Loop as Basic Element of Negative Permeability Meta-material," 2002 32nd European Microwave Conference, Milan, Italy, 2002, pp. 1-4.
- [4] H. Guo, Z. Sun and P. Wang, "Multiple Frequency Band Channel Modeling and Analysis for Magnetic Induction Communication in Practical Underwater Environments," in IEEE Transactions on Vehicular Technology, vol. 66, no. 8, pp. 6619-6632, Aug. 2017.
- Technology, vol. 66, no. 8, pp. 6619-6632, Aug. 2017.

 [5] H. Guo, and Z. Sun, "Full-duplex Metamaterial-enabled Magnetic Induction Networks in Extreme Environments," IEEE International Conference on Computer Communications (INFOCOM), Honolulu, HI, Apr. 2018.
- [6] E. Bou, R. Sedwick and E. Alarcon, "Maximizing efficiency through impedance matching from a circuit-centric model of non-radiative resonant wireless power transfer," 2013 IEEE International Symposium on Circuits and Systems (ISCAS2013), Beijing, 2013, pp. 29-32.
- [7] E. M. Thomas, J. D. Heebl, C. Pfeiffer and A. Grbic, "A Power Link Study of Wireless Non-Radiative Power Transfer Systems Using Resonant Shielded Loops," in IEEE Transactions on Circuits and Systems I: Regular Papers, vol. 59, no. 9, pp. 2125-2136, Sept. 2012.
- Systems I: Regular Papers, vol. 59, no. 9, pp. 2125-2136, Sept. 2012.
 [8] J. N. Murphy and H. E. Parkinson, "Underground mine communications," in Proceedings of the IEEE, vol. 66, no. 1, pp. 26-50, Jan. 1978.
- [9] H. Guo, Z. Sun, J. Sun and N. M. Litchinitser, "M²I: Channel Modeling for Metamaterial-Enhanced Magnetic Induction Communications," in IEEE Transactions on Antennas and Propagation, vol. 63, no. 11, pp. 5072-5087, Nov. 2015.
- [10] S. S. Mohan, M. del Mar Hershenson, S. P. Boyd and T. H. Lee, "Simple accurate expressions for planar spiral inductances," in IEEE Journal of Solid-State Circuits, vol. 34, no. 10, pp. 1419-1424, Oct 1999.
- [11] [Online]. Available: www.comsol.com